*Corresponding author; email: egutsmie@e18.physik.tu-muenchen.de

Understanding of Ultra-Cold Neutrons Production in Solid Deuterium.

A. Frei,[1] E. Gutsmiedl*,[1] C. Morkel,[1] A.R. Müller,[1] S. Paul,[1] S. Rols,[2] H. Schober,[2] and T. Unruh[3]

[1]*Technische Universität München,Physik Department,*
James Franck Str., D-85747 Garching, Germany
[2]*Institut Laue Langevin, 156X, F-38042 Grenoble CEDEX, France*
[3]*Technische Universität München,Forschungsneutronenquelle Heinz*
Maier-Leibnitz (FRM II), Lichtenbergstr. 1, D-85747 Garching, Germany
(Dated: June 17, 2010)

Our recent neutron scattering measurements of phonons and other quasi-particle excitations in solid deuterium (sD_2) and the extraction of the density of states for phonons and rotational transitions in sD_2 have led us to a new understanding of the production of ultra-cold neutrons (UCN) in sD_2. The UCN production rate reaches a maximum at an equivalent neutron temperature of T_n=40 K for a neutron flux with Maxwellian energy distribution. The cross section for UCN production in sD_2 has been determined by using the density of states $G_1(E)$ in combination with the incoherent approximation as well as by a direct calibration of our measured neutron cross sections with the known cross section of the $J = 1 \mapsto 0$ rotational transition in deuterium. Using this cross section we deduced the production rate of UCN in sD_2 which agrees quite well with direct measurements of this energy averaged UCN production cross section.

Ultra-cold neutrons (UCN) are slow enough to be confined [1] in traps, which can be formed by materials with a high Fermi potential (up to 300 neV) or by a magnetic field (60 neV/T). UCN can be observed for several tens of minutes in these traps, and are excellent tools for high precision measurements, as the life time of the neutron itself [2, 3], and the search for a possible electric dipole moment of the neutron [4] (current upper limit $2.9 \cdot 10^{-26}$ e· cm).

Powerful UCN sources are needed for the here mentioned experiments, and different groups [5–8] are working on the development of strong sources, based on sD_2 as an converter for down-scattering of thermal or sub-thermal neutrons into the UCN energy region (typical E <300 neV). A converter based on sD_2 should be operated at temperatures below T<10 K in order to avoid subsequent upscattering of UCN by phonons within solid deuterium [9]. The understanding of the downscattering of neutrons into the UCN region crucially relies on a detailed knowledge of the energy loss of thermal or subthermal neutrons in the sD_2 converter material. One major reaction channel is based on phonons in the solid deuterium crystal, which are excited by the neutrons.

We have recently measured the phonon system in sD_2 by neutron time-of-flight measurements at the IN4 (ILL Grenoble) and at the TOFTOF (FRM II, Munich). These measurements are described in detail in another paper [10].

Fig. 1 shows two examples of our neutron scattering data (angular averaged) for two different concentrations c_o of ortho-D_2 molecules. On the side of energy gain of the neutrons (positive E) we can identify the rotational transition $J = 1 \mapsto 0$. The intensity of this peak decreases with reduced para-D_2 molecule concentration $c_p = 1 - c_o$. A similar rotational transition (the $J = 0 \mapsto 1$ transition) can also be observed on the neutron energy loss side. Furthermore it is remarkable that the elastic cross section (E =0 meV) of sD_2 is quite large. Our data indicates that the elastic cross section makes up approximately 50% of the total cross section at thermal neutron energy. Another interesting feature is the neutron scattering intensity on the neutron energy gain side close to the elastic peak (E=0 meV). An increase of the concentration of the para D_2 molecules leads to a larger neutron up-scattering close to the elastic line. The origin of this cross section is very likely induced by phonons, which are interlinked with the rotational transitions $J = 1 \mapsto 0$ of the para molecules. This up-scattering has serious implications to the up-scattering of UCN in the sD_2 converter material, and reduces the achievable density of UCN in sD_2. A detailed analysis of these effects will presented in a forthcoming paper.

In addition the scattering function $S(Q,E)$ is shown for fixed values of momentum transfer Q in fig. 2. The dynamical scattering function $S(Q,E)$ comprises the phonon branches of the hcp-sD_2 [11] crystals and the $J = 0 \mapsto 1$ rotational transition. The acoustical phonons (transversal and longitudinal) are clearly visible in $S(Q,E)$ while the optical phonon branches are not. The rotational transition $J = 0 \mapsto 1$ shows a significant Q - dependence and it is purely incoherent. The position the $J = 0 \mapsto 1$ transition peak (E_{01}=7.4 meV) does
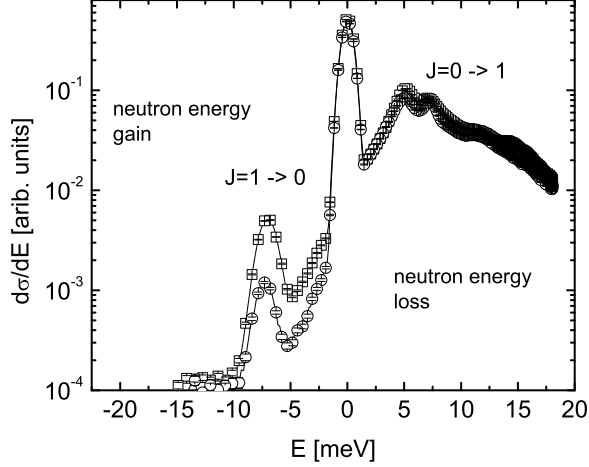
FIG. 1: An example of a dynamical neutron cross section of solid D_2 at $T = 7$ K. Comparison of two ortho concentrations c_o=66.7% (□) and c_o=98% (○). Data from TOFTOF measurements at the FRM II. Initial energy of the thermal neutrons is E_0=20.4 meV.

not change much at different Q-values. The cross section $d\sigma_{J=0\mapsto 1}/d\Omega$ for this transition is shown in fig. 3. This cross section was extracted from our data by a integration of S(Q,E) at E_{01}=7.4 meV with a width of ΔE= 1meV at different Q-values. The Q-dependence of this cross section was fitted using the incoherent scattering length of the $J = 0 \mapsto 1$ transition [10]

$$\frac{d\sigma_{J=0\mapsto 1}}{d\Omega}(Q) \sim j_1^2(Qa_s/2) \cdot e^{-\frac{1}{3}Q^2\langle u^2\rangle}. \qquad (1)$$

The parameter $a_s = 0.74$ Å is the distance of the deuterons within the D_2 molecule, while $\langle u^2\rangle$ is the mean square displacement of the D_2 molecule in the lattice. The form factor j_1 for the $J = 0 \mapsto 1$ transition is described by a spherical Bessel function of first order. The result for $\langle u^2\rangle \simeq 0.245 \pm 0.02\text{Å}^2$ is in good agreement with earlier published results [11]. The peak-like deviations in fig. 3 at certain Q-values are the result of coherent neutron scattering on phonons.

With the aid of our neutron data we are able to determine the UCN production cross section by two ways. One way is the determination of the quasi-particle (phonons and rotational excitations of the D_2 molecules) density of states $G_1(E)$. The other way is the direct integration of the dynamical neutron cross section in the kinematical region along the free neutron dispersion parabola.

With the knowledge of the quasi-particle density of states $G_1(E)$ it is possible to calculate the dynamical

neutron cross section $\frac{d\sigma}{dE_f}$ (averaged over the scattering angle, thus Q). Vice versa it is also possible to extract $G_1(E)$ from a measured $\left[\frac{d\sigma}{dE_f}\right]_{data}$ using *Turchin's* theory [12] for this cross section applying the incoherent approximation. The absolute normalization of $\left[\frac{d\sigma}{dE_f}\right]_{data}$ is not needed, because the extracted $G_1(E)$ has to be normalized to unity anyway. This approach is only valid within the Born-approximation.

The method of determination of $G_1(E)$ from our data is described in [10] in detail. Contributions of higher order multiphonons to $\frac{d\sigma}{dE_f}$ are incorporated.

The result of our analysis [10] concerning $G_1(E)$ and a comparison with a Debye model is shown in fig. 4. The characteristics of $G_1(E)$ was already discussed in detail in [10] but it is worth to summarizing these results again, because they have an important impact on the UCN production cross section. One major feature is the occurrence of these excitations above E~10 meV in the one-quasi-particle density of states $G_1(E)$. These excitations above E~10 meV are depending on the concentration of ortho-D_2. The optical phonons in the region of E [8-10 meV] are not clear visible in $G_1(E)$.

In the case of UCN production the energy transfer of the down-scattered neutron $E = E_0 - E_f$ is approximately equal to the initial neutron energy E_0 ($E_f = E_U \ll E_0$, E_U: UCN energy).

The total cross section for UCN production can be calculated by

$$\sigma_{UCN}(E_0) = \int_0^{E_U^{max}} \frac{d\sigma(E_0)}{dE} dE_U \qquad (2)$$

and is shown in fig. 5. It can be compared with recent published data of the UCN group at the PSI [13] which has studied UCN production at a cold neutron beam ($E_0 \sim$1.4 meV to 20 meV). The agreement of data and our calculation, using our data for $G_1(E)$ and *Turchin's* incoherent approximation is surprisingly good. The calculated cross section comprises the contribution of one-quasi-particle and two-quasi-particle excitations. Three-quasi-particle excitations do not appear below E~14 meV (see fig. 9 in [10]) and are rather small in their contribution. The authors of [13] compared their results to a calculated cross section based on a multi-phonon Debye model. They also reported, that using a 'more realistic model' for the density of states (*Yu et al.* [11, 17]) leads to a considerably worse fit of their data. Using a Debye model with a cut-off at $k_B \cdot \Theta_D$ =9.5 meV (Debye temperature Θ_D=110 K) only the contribution of two-phonon excitation have to be included in order to fit the measured cross section of σ_{UCN}=1.55 10^{-7} barn at E=14.7 meV [13]. This also applies for the density of states model of *Yu et al.*. Our own calculated cross section shows a

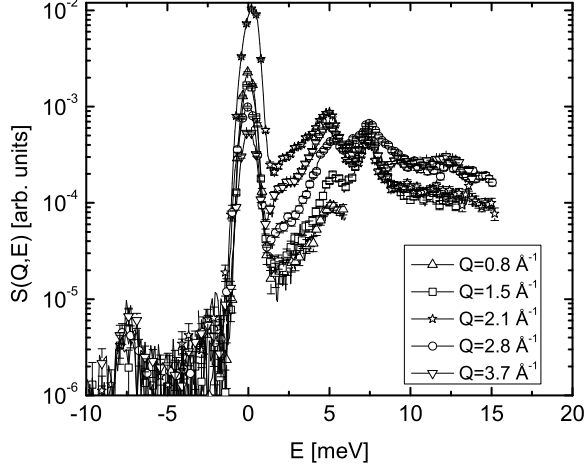FIG. 2: $S(Q,E)$ of sD$_2$ for $c_o = 95.2\%$ at $T = 4$ K for different fixed values of Q. Data from IN4 measurements.

FIG. 3: Cross section $d\sigma_{J=0\mapsto 1}/d\Omega$ of sD$_2$ for c_o=95.2% o-D$_2$. ■ - Data from IN4 measurement. Black line - Fit result using eq. 1.

combination of one-quasi-particle and two-quasi-particle excitations contributing at these energies. In detail our data indicate (see fig. 5) that the UCN production cross section is mainly determined by one-quasi-particle excitation for energies below E=15 meV (see fig. 4). Even though the two-quasi-particle contribution can not be neglected in the region of E 5-25 meV.

The application of the incoherent approximation in the case of sD$_2$ has certainly to be questioned. The sD$_2$ crystal scatters neutrons more coherently than incoherently. This fact leads to the question: Is it possible to get the UCN production cross section directly from the neutron scattering data?

The easiest way of determining the cross section for UCN production is the use of the dynamical scattering function $S(Q, E = \frac{\hbar^2}{2m}Q^2)$ in the (Q, E)-phase space along the free neutron parabola (dispersion curve with $E \simeq E_0 = \frac{\hbar^2}{2m}k_0^2$ and $Q \simeq k_0$). This approach equally rely on the Born approximation. The UCN production cross section can be determined by

$$\sigma_{UCN}(E_0) = \frac{\sigma_0}{k_0}S(k_0, \frac{\hbar^2}{2m}k_0^2)\frac{2}{3}k_U^{max}E_U^{max}. \qquad (3)$$

The term $E \simeq E_0 = \frac{\hbar^2}{2m}k^2$ is the energy of the incoming neutron in the down-scattering process, while k_U^{max} and E_U^{max} are the upper limits for the UCN momentum and energy. In order to obtain absolute cross sections the dynamical scattering function of solid deuterium extracted from our neutron scattering data has to be calibrated to absolute values. This can be done by using the rotational transition $J = 1 \mapsto 0$ as reference process for calibration. The cross section for the $J = 1 \mapsto 0$ transi-
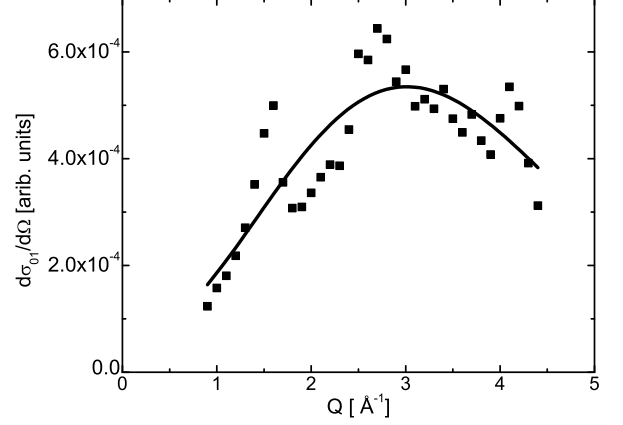
tion was calculated by *Hamermesh* and *Schwinger* [14] for ortho- and para- deuterium molecules (gas). These calculation include also thermal movements (maxwellian distribution of velocities) of the deuterium molecules in the gas. The application of these calculations to the rotational transitions of the D$_2$ molecules, which are pinned in a crystal at fixed positions may of course be questionable. However the rotational transitions in sD$_2$ are not very much hindered by the crystal binding of the crystal [15]. Indeed the molecules are of course not at rest, they perform motions around their equilibrium positions. These movements are caused by the zero-point-motions and also by existing phonon excitations in the crystal. A similar problem was considered by *Lamb* [16] in the past. He calculated the capture of neutrons by atoms in crystals. His calculations for crystals with weak lattice binding delivered the finding, that atoms in such crystals can be treated as a gas with an effective temperature, which depends on the Debye temperature of the crystal. This effective temperature can be higher than the real temperature of the solid and is just a result of the average energy of the vibrational degrees of freedom plus the zero-point-motion. We used this ansatz to calculate the effective temperature ($T_{eff} \simeq$40 K at a deuterium temperature of 4 K) of the D$_2$ molecules and used it for the calculation of the rotational transition ($\sigma_{J=1\mapsto 0}$) of our quasi free molecules, following the theory of *Hamermesh* and *Schwinger*.

The cross section $\sigma_{J=1\mapsto 0}$ in pure para deuterium has a value of $\sigma_{J=1\mapsto 0}$=0.61 barn for E_0=17.2 meV (corresponding to the energy of the incoming neutrons at the IN4 experiment) at a deuterium temperature of T=4 K. The comparison of our neutron scattering data of natural deuterium (c_O=66.7%) and ortho enriched deuterium
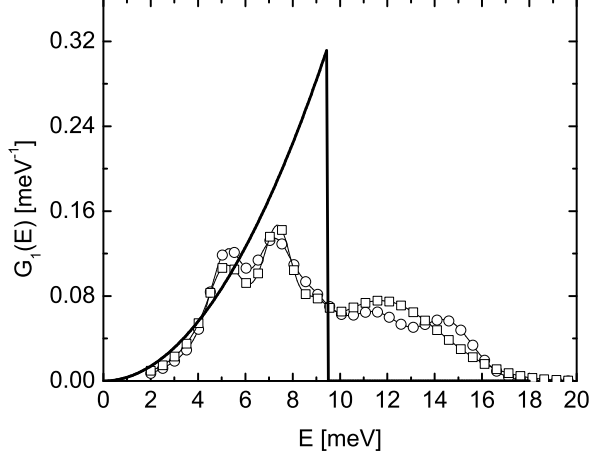
FIG. 4: Comparison of the one-quasi-particle density of states of solid D_2 for $c_o = 66.7\%$ ($\bigcirc$) and $c_o = 98\%$ ($\square$) at $T = 7$ K with a Debye model (line). Data from TOFTOF measurements (energy resolution: $\Delta E \sim 1.24$ meV). The sD_2 poly crystal is prepared by fast freezing (several minutes) of liquid D_2 down to a temperature of $T < 10$ K. $\int_0^\infty GDOS(E) \cdot dE = 1$

FIG. 5: UCN production cross section of $c_o = 98\%$ solid D_2. UCN energy range 0-150 neV inside the solid D_2. Solid line - cross section calculated in incoherent approximation, using $G_1(E)$ from [10]. Dashed line: one-quasi-particle contribution. Dotted line: two-quasi-particle contribution. $\square$ - data from measurements at the PSI [13].

indicated a ortho concentration of $c_O=(95.2 \pm 0.3)\%$.

Scaling with the para concentration of our sample ($c_P = 1 - c_O = 4.8\%$) thus leads to a value of $\sigma_{J=1\mapsto0} = 0.029$ barn for our ortho enriched solid D_2 sample. This value for $\sigma_{J=1\mapsto0}$ can be used to calculate a scaling factor for $S(Q,E) = \kappa \cdot S_{data}(Q,E)$.

By means of this value it is possible to calculate the total neutron scattering cross section for $E_0=17.2$ meV neutrons: $\sigma_{tot}(E_0=17.2$ meV$)=23.4$ barn. The assumption is of course only valid, if the kinematical area of our neutron scattering experiment covers most of the possible scattering processes. A good cross check of this value is the calculated value for the total cross section for solid poly-crystalline deuterium, using the incoherent approximation of *Turchin* [12].

The result of this calculation leads to a value of $\sigma_{tot}(E_0=17.2$ meV$)=23.8$ barn, which is close to the value of our calibration. The dynamic response function $S(Q,E)$, resolved from our data analysis, was not corrected for multiple scattering effects. Therefore the estimated error of this calibration is approximately 12% [20]. The result of this calibration and determination of the UCN production cross section as function of the the energy of the incoming neutrons, and a comparison with measurements of this cross section [13] is shown in fig. 6. The agreement of the absolute values of the measured cross section with the resolved values form our $S(Q,E)$ data is reasonable. The comparison of the calculated UCN production cross sections, extracted from the inco-
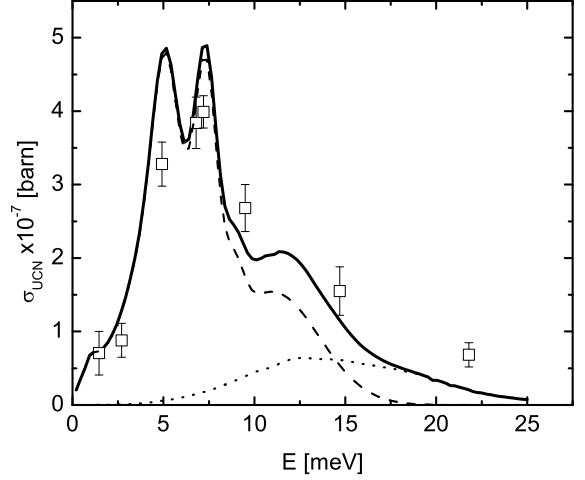
herent approximation and parabola method shows (see fig. 5 and fig. 6) a discrepancy in the region of $E \sim 6$ meV. The cross section, determined by the parabola method exhibits a pronounced maximum in the region of $E \sim 6$ meV as compared to the incoherent approximation result.

In fig. 7 the dynamical scattering function $S(Q,E)$ (neutron energy loss side) of fast frozen solid ortho-deuterium is shown. The black line corresponds to the dispersion of the free neutron.

The parabola of the free neutron crosses the acoustical phonon dispersion curve at $E \sim 6$ meV(see fig. 7). At this point, the UCN production cross section is predominantly determined by coherent scattering. This can explain a deviation from the production cross section in incoherent approximation. Nevertheless the general agreement of the incoherent approximation with the PSI data is remarkable (see fig. 5)

The effective UCN production rate P (UCN cm^{-3} s^{-1}) from a neutron beam is determined by integrating the product of the UCN production cross section $d\sigma/dE$ and the spectral flux $d\Phi/dE$ (Maxwell spectrum with effective neutron temperature T_n) of the incoming neutrons over the finite UCN energy range (E_U^{max} maximum allowable UCN energy) and over the energy spectrum of the incoming neutron, still assuming $E = E_0$.

$$P(T_n) = N_{D_2} \cdot \int_0^{E_U^{max}} \int_0^{E^{max}} \frac{d\Phi(T_n)}{dE_0} \cdot \frac{d\sigma}{dE_0} dE_U dE_0. \quad (4)$$
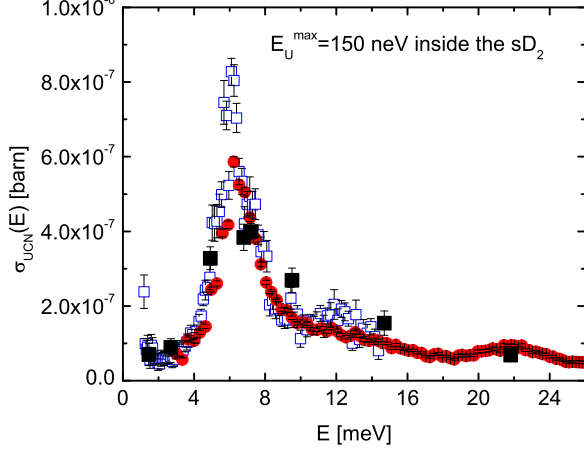
FIG. 6:

UCN production cross section solid D_2 of $c_o = 95.2\%$. A UCN energy range of 0-150 neV inside the solid D_2 is assumed. Cross section determined by an integration of $S(Q,E)$ along the free dispersion of the neutron (sample - fast frozen solid deuterium ($T = 4$ K)); data from IN4 measurements. Blue $\square$ - $E_0 = 17.2$ meV. Red filled $\bigcirc$ - $E_0 = 67$ meV, [18]. $\blacksquare$ - direct UCN production data from measurements at the PSI [13]. The PSI data do not show a distinct peak at $E \sim 6$ meV
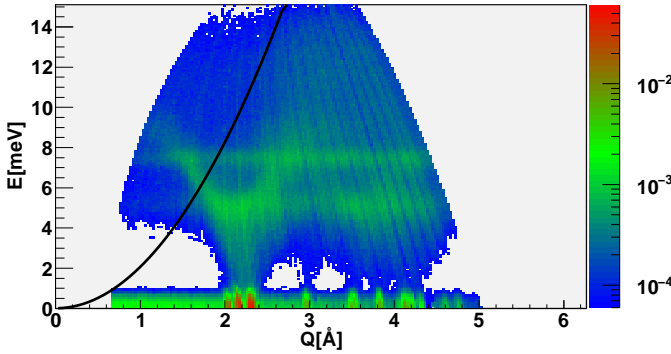

FIG. 7:

$S(Q,E)$ of sD_2 for $c_o = 95.2\%$ at $T = 4$ K. Data from IN4 measurements. Black parabola - dispersion of the free neutron.

In fig. 8 the result for the UCN production rate in solid ortho deuterium, exposed to Maxwellian shaped neutron flux for different effective neutron temperatures is shown, using eq. 4.

The main conclusion from these results is the new understanding of possible higher energetic loss channels (one-quasi-particle and two-quasi-particle excitations) in solid deuterium for the down scattering of thermal or cold neutrons in the conversion process to UCN. The best value for the effective neutron temperature is in the region of $T_n \sim 40$ K, which is larger than the value
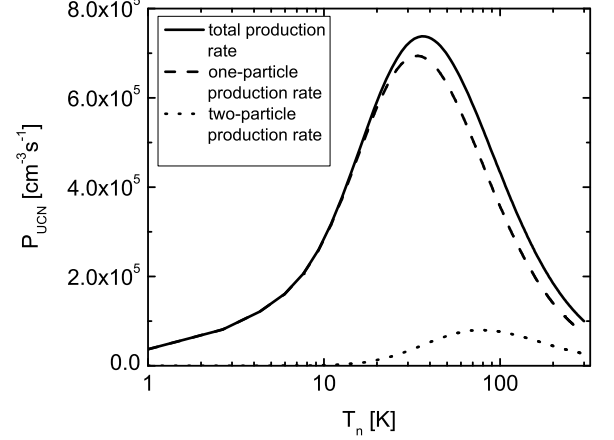

FIG. 8: Calculated UCN production rate of $c_o = 98\%$ solid D_2 for different Maxwellian neutron spectra with effective neutron temperature T_n. UCN energy range - 0-150 neV inside the solid D_2. Neutron capture flux $\Phi_C = 1 \cdot 10^{14}$ cm^{-2} s^{-1}. Solid line - total production rate (one- and two particle excitation). Dashed line - one-particle production rate. Doted line - two-particle production rate.

($T_n \sim 30$ K) reported by Yu et al. [17] in an earlier publication. A similar result was obtained by Serebrov et al. [19] using a Debye-model for sD_2 in a theoretical calculation, based on the incoherent approximation. The agreement of our result with the results of the calculation applying a Debye-model is not a surprise, because they include mulit-phonon excitations in their calculations, while Yu et al. considered only one-phonon excitations.

In summary, new neutron scattering data of solid deuterium leads to a better understanding of UCN production in this converter material. The new results for the density of states in sD_2 and the results for the UCN production cross section, extracted directly from the dynamical scattering function $S(Q,E)$ predict a significant UCN production cross section for incoming neutrons with energies higher than $E_0 > 10$ meV. This observation was also confirmed [13] by direct measurements of the UCN production cross section. An optimized sD_2 UCN source should be exposed to a cold neutron flux with an effective neutron temperature of $T_n \simeq 40$ K.

[1] R. Golub, D. Richardson, S.K. Lamoreaux, Ultra-Cold Neutrons, Adam Hilger,Bristol, Philadelphia and New York (1991).

[2] S. Arzumanov et al., Phys. Lett. **B 483**, 15 (2000).

[3] A. Serebrov et al., Phys. Lett. **B 605**, 72 (2005).

[4] C. A. Baker et al., Phys. Rev. Lett. **97**, 131801 (2006).

[5] A. Frei et al., EPJ **A 34**, 119 (2007).

[6] Roger E. Hill et al., Nucl. Instrum. Methods Phys. Res. **A 440**, 674 (2000).

[7] A. Anghel et al., Nucl. Instrum. Methods Phys. Res. **A 611**, 272 (2009).

[8] A. Serebrov et al., JETP Lett. **62**, 785 (1995).

[9] C.-Y. Liu et al., Phys. Rev. **B 62**, R3581 (2000).

[10] A. Frei et al., Phys. Rev. **B 80**, 064301 (2009).

[11] M. Nielsen and H. Bjerrum MØller, Phys. Rev. **B 3**, 4383 (1973).

[12] V.F. Turchin, Slow Neutrons, Israel Program for Scientific Translations,Jerusalem, (1965).

[13] F. Atchison et al., Phys. Rev. Lett. **99**, 262502-1 (2007).

[14] M. Hamermesh and J. Schwinger, Phys. Rev. **69**, 145 (1946).

[15] J. van Kranendonk and G. Karl, Rev. Mod. Phys. **40**, 531 (1968).

[16] W.E. Lamb Jr., Phys. Rev. **55**, 190 (1939).

[17] Z-Ch. Yu, S. S. Malik and R. Golub, Z. Phys. B **62**, 137 (1985).

[18] The calibration of $S(Q, E)$ at this energy was done by using the calculated total cross section $\sigma_{tot}(E_0 = 67 \text{ meV})$ in incoherent approximation.

[19] A. Serebrov et al., JETP Lett. **59**, 757 (1994).

[20] The treatment of multiple scattering effects in our solid deuterium samples are discussed in detail in ref. [10].